Available online at www.sciencedirect.com

ScienceDirect

Procedia CIRP 108 (2022) 839–844

www.elsevier.com/locate/procedia

6th CIRP Conference on Surface Integrity

The influence of surface finishing on laser heat treatments of a tool steel

J N Lagarinhos[a,b*], S Santos[c], G Miranda[b,c], D Afonso[a,d], R Torcato[a,b], C Santos[e] and J M Oliveira[a,b]

[a]*EMaRT Group – Emerging: Materials, Research, Technology, School of Design, Management and Production Technologies, University of Aveiro, Estrada do Cercal 449, 3720-509 Oliveira de Azeméis, Portugal.*
[b]*CICECO – Aveiro Institute of Materials, University of Aveiro, Campus Universitário de Santiago, 3810-193 Aveiro, Portugal.*
[c]*Department of Materials Engineering and Ceramics, University of Aveiro, Campus Universitário de Santiago, 3810-193 Aveiro, Portugal.*
[d]*TEMA – Centre for Mechanical Technology and Automation, Mechanical Engineering Department, University of Aveiro, Campus Universitário de Santiago, 3810-193 Aveiro, Portugal.*
[e]*Macro-Moldes Para Plásticos Lda, 3720-917 Oliveira de Azeméis, Portugal.*

* Corresponding author. Tel.: +351256666960; *E-mail address:* joanalagarinhos@ua.pt

Abstract

Laser heat treatments (LHT) has received growing attention in the last years because of highly localized precision and manufacturing efficiency related to laser processing of moulds steel. Due of its strong resistance and ability to maintain hardness and strength at high temperatures, AISI P20 steel is one of the most widely used tool steel in the plastics injection mould industry.
This work presents an experimental investigation on LHT using P20 mod. steel produced with different surface finishes. After mechanical surface finishing, the diode laser beam with 15 mm width was applied to the P20 specimens at 1060 ºC using a feed rate of 8.8 $mm{\cdot}s^{-1}$in an air and argon ambient. The influence of different LHT atmosphere conditions and specimen initial surface finishing on characteristics such as final roughness, microhardness and microstructure were comprehensively analyzed. The use of a controlled atmosphere during processing showed an increment in depth and hardness values of samples. Through 3D profilometer, it was possible to determine the samples roughness. Results showed that lower average roughness leads to higher hardness values close to the surface, while higher average roughness lead to a deeper heat-treated zone. Macroscopical analysis revealed the depth and width afftected by LHT. The microhardness results showed an increment from 300 HV to around 750 HV on laser heat-treated zone using a controlled environment. Optical microscopy analysed the microstructural changes into martensite between LHT and non LHT zones for all samples.

Keywords: Laser; local heat treatments; surface finishing

1. Introduction

The constant evolution of the plastic injection industry market demands that high productivity and quality of molds is achieved [1]. Due to the continuous rise in plastic products mass production, these tools are exposed to thermo-mechanical loads that negatively influences the surface of molds steel [2]. Therefore, the necessity to develop mold steel with superior durability has arisen. Several methods have been applied to enhance the lifetime of a mold tool and to improve the final properties. The surface quality is a characteristic that also needs to be considered.

Laser-based surface treatments is an effective method to increase the final properties of a mold metallic part [3]. The most common lasers used in industry are high power diode laser [4–7], CO_2 [8] and laser Nd: YAG (Neodymium doped yttrium aluminum garnet) [9]. Among these, the high power diode laser is particular suitable for surface properties treatments of mold steels due have smaller wavelength that allows for a higher absorption rate in steels. [7,10]. Using diode lasers have possibility to achieve highest depths using less energy once

10.1016/j.procir.2022.03.129

wavelength range of the laser beam is well absorbed by the metal. A higher work efficiency is also possible to obtain using high power diode lasers compared to another surface modification processes as gas nitriding, plasma nitriding, chemical vapor deposition [7,11,12]. Laser based surface treatments are mostly performed in air conditions with absence of a controlled environment. However, using air without any controlled environment can be less effective for steels, as in low carbon content oxidation phenomenon can negatively affect the hardening process [13]. Laser heat treatments (LHT) under a controlled atmosphere can be a solution to improve surface hardness. The incorporation of an inert gas environment during experiments can improve both the mechanical and tribological properties of steels [14,15].

AISI P20 mod. steel is a commercial mold steel commonly used in injection mold industry, due to its good mechanical properties, machinability, and easy polishing. Previous research on the study of the LHT effect on hardness of tool steels was carried out and the results have shown a 108% increase in hardness steel after inducing by LHT [3].

In this study, laser heat treatments using a high power laser were applied on AISI P20 with a special attention for the influence of different surface finishes to obtain high durability of steel for injection mold application. LHT under air and controlled conditions were also evaluated.

2. Experimental Procedure

2.1. Materials

For the experimental studies, a set of five samples of AISI P20 modified was selected to study the influence of different surface finishes. Table 1 summarizes the chemical composition of the material used in this study.

Table 1. Chemical composition of the P20 mold steel (wt.%) [16].

Steel	Mn	Cr	C	Si	Mo	P
P20 mod.	1.53	1.9	0.4	0.24	0.22	0.01

2.2. Samples preparation

Parallelepipedal samples of P20 tool steel with dimensions of 85 (W) x 50 (D) x 22 (H) mm were prepared to obtain five different surface finishes (Fig. 1).

A rough milled sample (RM) was obtained using a 5-axis universal CNC machine equipped with a 32mm diameter milling head (MQX-5032-M16) with cutting inserts (EPMT100312ZER). Two other samples were equally machined and then brushed using a 6-axis robot equipped with a 75mm diameter x 6mm ceramic brush (3M Scotch Brite BB-XS-120). The brushed sample 1 (B1) undergo one brush passage and the brushed sample 2 (B2) featured three brush passages in perpendicular directions. A finishing milling sample (FM) was obtained using the 5-axis universal CNC machine equipped with a 2mm diameter ball nose CBN tool (XBO20420-4-11G), getting an even finishing, characterized by regular height and shape crests. The polished sample (P) was achieved with a KK114F (VSM) sandpaper with a particle size of P320 and then a CP918A (VSM) with a particle size P800.

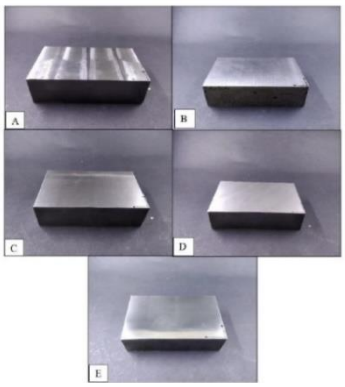

Fig. 1. Samples obtained after surface finishes: a) Rough milling (RM); b) Brushed 1 (B1); c) Brushed 2 (B2); d) Finish milling (FM) and e) Polish (P).

2.3. Experimental setup for laser heat treatments

Laser heat treatments (LHT) were conducted with a LDF 4500-60 diode laser from LASERLine, incorporated in an ABB IRB 6700 robot. The rectangular spot size was fixed in 15 mm by 7.2mm and a continuous laser beam up to 4.5 kW with a combined wavelength from 960 nm and 1020 nm diode emitters was applied.

The rectangular laser beam moved in a single linear path with a transverse scanning motion was applied in the central part of the samples, along ~ 55 mm. The temperature used in experiments was set to 1060 ºC with a scanning laser beam speed of 8.8 $mm \cdot s^{-1}$, based on results from previous studies [3]. A pyrometer was fixed on the laser head and measured the surface temperature of the sample controlling the laser power in real-time. Power usage averaged 45% of available power after temperature is stable. Fig. 2 presents the laser power usage and measured temperature for one sample LHT. Power curves were independent from the sample initial surface finishing or the use of protective atmosphere.

A chamber with dimensions of 120 (H) x 80 (W) x 55 (D) mm^3 was developed to conduct the LHT tests under inert conditions environment. Continuous pure argon (Ar) gas atmosphere with a 10 L/min flow was maintained during the LHT process. The results for both experiments were compared.

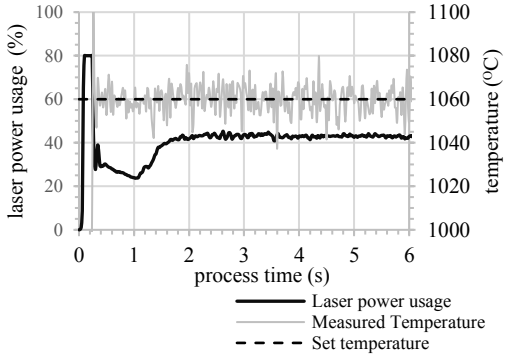

Fig. 2. Laser power usage and measured temperature during the LHT.

The parameters and treatment strategies to operate the laser, were found to be optimal in earlier studies using the laser [3].

2.4. 3D optical profilometry and roughness

A 3D optical profilometry equipment from *Sensofar S-neox* was applied to characterize the surface treated and untreated zones. The *SensoSCAN software* was used for analysis and visualization of the microtopography surface.

With this equipment, the different roughness parameters were verified, and the 3D topographies of the samples were recorded. The roughness parameters were calculated according to the ISO 25178 standard for multiscale 3D parametric assessment of surface topographies

2.5. Microhardness analysis

The microhardness tests were carried out to characterize the hardness of the samples cross-section and to measure the LHT depth. The samples were cut in the HAZ direction into small parallelepipeds of similar dimensions (~10x22x50 mm).

A Vickers microhardness tester from *Buehler*, model *Wilson VH1102* with an indentation load of 2kgf and a holding time of 10s was used. For each sample, several indentations were performed as a function of the depth and distance to the centre of the laser thermal treatment.

2.6. Microstructure and macrostructure analysis

A *ZEISS* optical microscope model *JENAPHOT2000* and a *Leica model EZ4HD* magnifying glass were used to analyse the microstructure of the treated and untreated zones. A 2% and 5% Nital etching solutions were used to reveal the microstructure by optical microscopy [17]. A magnifying glass was also used to observe the macroscopical separation on the treated zone.

3. Results and Discussion

3.1. 3D optical profilometry and roughness characterization

Profilometry analyses were performed on untreated and treated zones before and after argon gas use. For each sample, the roughness parameters were obtained. Fig. 3 represents the roughness results obtained for different samples. S_a is one of the most analyzed roughness parameters and corresponds to the arithmetic mean of the heights of the sample surface. S_z is the maximum height of the roughness profile.

Observing the results from Fig. 3 it was possible to observe that S_a parameter revealed an increase from untreated to treated zones in all samples treated without a protective atmosphere. The same behavior was also observed for S_z parameter, all samples presented a slightly increase in roughness.

Comparing the results obtained from experiments with and without argon gas, it was possible to conclude that in general the increase in roughness was not observed in all samples except P after laser treatments in a protective atmosphere.

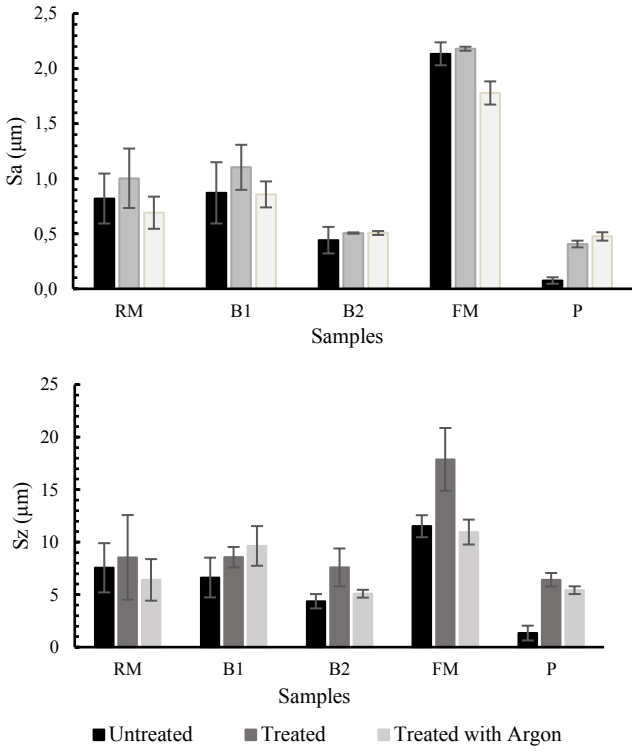

Fig. 3. Roughness parameters results of samples.

3.2. Microhardness results

The microhardness values after LHT were measured at different points of the sample and are demonstrated in Fig. 4. Indentations in depth (0.40 mm, 0.70 mm, 0.85 mm, 1.00 mm, and 1.15 mm) and as a function of the distance to the LHT centre (0mm, 3mm, 6mm and 9mm) were performed.

The microhardness profiles clearly showed the influence of the LHT on the cross-sectional areas of the samples. LHT under argon inert atmosphere produced a higher increment in hardness compared to LHT in air conditions.

The microhardness of the metal base P20 mod. steel was approximately 300 HV. In air conditions, it was observed an increment in hardness profiles from 300 HV to around 750 HV, within the quenching zone, that evidences a microstructural transformation after LHT. At 9 mm distance from laser centre no LHT effect is observed on testing piece hardness profiles. At 6 mm distance, the hardness decreased in the treated areas as function of depth. At 3 mm distance, an increase in depth was observed in experiments using argon, comparing to the experiments in air conditions. Maximum hardness values, calculated by the average of the 3 highest measured points, after LHT can be observed in Table 2.

The LHT reached between 0.7 and 0.85mm (± 0.05) depth without gas, and between 0.9 and 1.10mm (± 0.05) depth using an inert atmosphere, with all values presented in Table 3.

In all experiments, RM, FM, and P samples presented higher hardness values in the centre zone of sample, followed by a decrease until reaching the base metal hardness on the periphery of the treated area. A higher depth was also observed in these samples. The decreasing observed on the periphery area occurred due to the laser's energy distribution profile that flattens out at the edges of the spot. The results clearly

confirmed an increase of 120% (without gas) and 150% (with gas) for sample P on the hardness comparing to the metal base hardness before heat treatment. B1 and B2 samples showed the lowest hardness values, demonstrating that LHT was not effective using a brushed surface finish.

In general, the results clearly showed that maximum hardness and depth were more effective for experiments using argon gas. A possible explanation is related to argon use. Since that argon is an inert gas can prevent the surface from contact with air. The use of argon will avoid the occurrence of surface oxidation that is usually responsible for the weakness of the steel surface due to the presence cracks and voids [18].

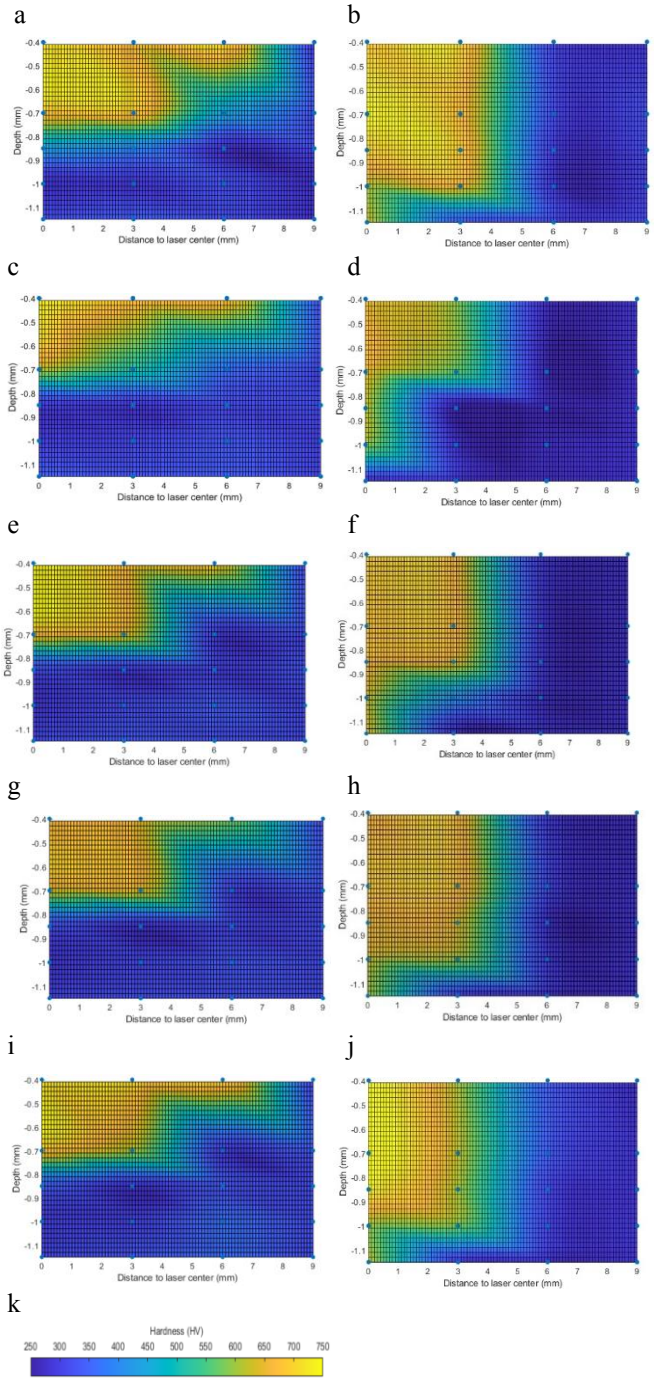

Fig. 4. Microhardness profiles of P20 steel samples: a), b) RM; c), d) B1; e), f) B2; g), h) FM; i) j) P; k) hardness scale. a), c), e), g), i) experiments without argon gas; b), d), f), g), j) experiments with argon gas.

Table 2. Maximum hardness from samples after LHT.

Sample	Average Hardness (HV) before LHT	Hardness (HV) LHT	Hardness (HV) LHT with argon gas
RM		680 ± 14	706 ± 14
B1		640 ± 19	705 ± 39
B2	306 ± 28	685 ± 12	701 ± 37
FM		716 ± 25	653 ± 12
P		763 ± 26	719 ± 3

3.3. Optical and macroscopical analysis

The microstructure was investigated by optical microscopy analysis to analyse the variations in hardness. The microstructure is dependent on the steel supply status and on the heat and cool cycles that occur during the LHT process. After chemical etching, no clear microstructural differences were observed between samples treated in air and argon conditions. The results for FM sample are showed to demonstrate the phase transformation within LHT zone.

Through the sizes indentation (Fig. 5a) it was possible to confirm the hardness values obtained within the LHT zone and non LHT zone. As microhardness profiles previously revealed, the indentations obtained on the LHT zone were smaller than those obtained in the non-treated zone. Fig. 5b presents the cross-sectional microstructures of the treated zone.

The typical martensite morphology transformation was detected within the LHT. This morphology is characterized by a metastable phase that results from rapid cooling and generates an increment in surface hardness [19].

Using a magnifying glass, it was possible to observe macroscopically the depth and width reached by LHT after chemical etching (Fig.6).

Table 3 presents the results obtained concerning the depth reached in the centre of the samples by the LHT. The values were obtained using ImageJ software [20].

The depth of the heat-treated zones was affected according to the surface finish of the samples. As previously mentioned, the experiments using argon gas it was observed the highest increment in depth. The maximum depth increased from 0.893 ± 0.005 mm on LHT to 1.181 ± 0.005 mm using argon during LHT. During LHT, FM sample presented the highest depth value. When argon gas was used, the highest deep was achieved for P and RM samples.

As observed in Table 3, the width results obtained were smaller than the laser spot, indicating that the entire area of the laser is not useful. This is due to the peripheral flattening of the laser's energy distribution.

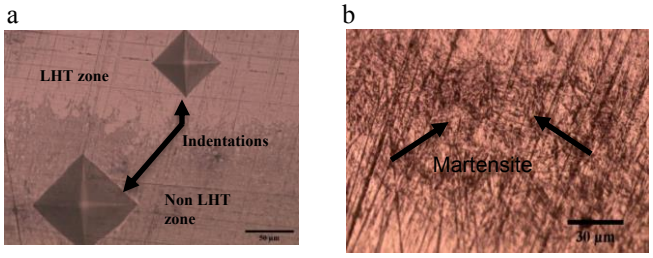

Fig. 5. Optical microscopy images (a) indentations performed on LHT and non LHT zones; (b) martensitic microstructure present in LHT zone.

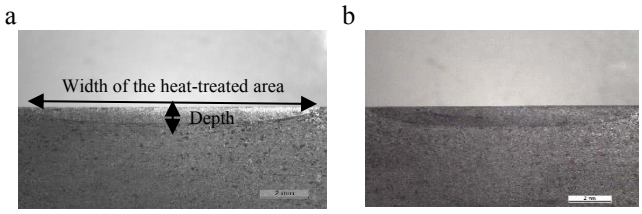

Fig. 6. Macroscopic images (a) after LHT (b) after LHT with argon.

Table 3. Depth and width reached by LHT and LHT with gas in samples.

Sample	Depth x Width (mm) LHT	Depth x Width (mm) LHT with argon gas
RM	0.885 x 12.745	1.178 x 13.803
B1	0.871 x 12.654	1.050 x 13.629
B2	0.864 x 12.651	1.091 x 13.773
FM	0.893 x 12.727	1.156 x 13.642
P	0.852 x 12.607	1.181 x 13.480

*(± 0.005) for all samples.

This behaviour is similar to a previous study and demonstrates that increasing roughness, improves the laser absorption, which will increase the effectiveness of the LHT without a protective atmosphere [21]. As observed in Fig. 7, the same behaviour is not as clear when LHT with argon gas.

The laser absorption is affected by surface reflectivity, which suggests that higher roughness leads to a lower reflectivity, and consequently an increase in absorption.

4. Conclusions

This work allowed to obtain deeper knowledge about different surface finishes of P20 mod. steel using LHT with and without a controlled atmosphere.

From the results obtained by 3D profilometry, it was possible to observe that LHT increases the roughness of different samples. However, the machining cresses were reduced when the laser passes. This reduction is mostly evident in the samples centre. Using protective gas, the results showed a decrease in samples roughness. It was concluded that the use of protective gas can lead to a decrease in samples roughness for initial surface finishes greater than Sa 0,5µm.

The effect of LHT in hardness demonstrates that the polished sample has the highest hardness value, reaching 720 HV. The surface hardness increased from around 300 to 700 HV, between the treated and untreated zones. For experiments using argon a higher hardness and deeper were achieved during LHT. Macroscopic analyses also corroborated this result. The depth increased from 0.85 to 1.18 (± 0.05) and revealed the effect of LHT using a protective gas. Through optical microscopy, it was observed a microstructural change into martensite between LHT and non LHT zones for all samples.

Based on this study results, it was possible to conclude that, regarding hardness, decreasing roughness increases the LHT efficiency. The opposite is observed regarding the reachable depth. It was also possible to conclude that the use of a controlled atmosphere during experiments led to higher effectiveness on LHT. This is due to the presence of argon gas that can prevent the surface from contact with air, and consequently the occurrence of surface oxidation. As previously mentioned, the surface oxidation is responsible for

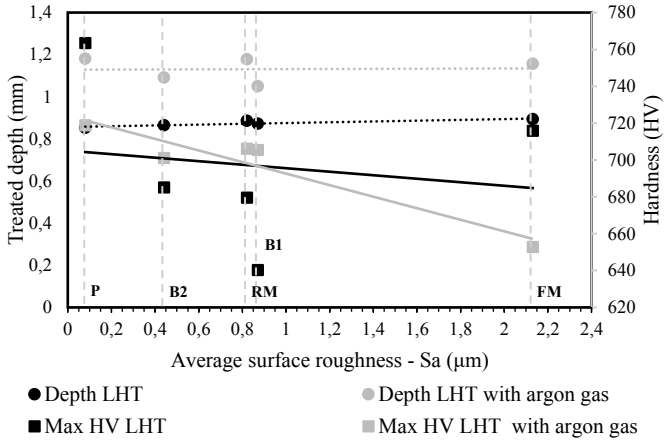

Fig. 7. Relation between surface roughness and LHT depth and hardness.

cracks and voids that will influence the surface hardness of steels.

For plastic injection moulds applications, it is suggested the use of a polish surface finish for the optimal pre-processing conditions. Injection moulds with this surface state and heat-treated by using a high-power diode laser under controlled atmospheric conditions can improve the life of AISI P20 mod. tool steel.

Acknowledgements

The authors would like to acknowledge the financial support from Laser4AMTT project. This is a project in collaboration with Macro Moldes para Plásticos Lda and co-financed under Portugal 2020 and European Regional Development Fund, through COMPETE under the scope of the project POCI-01-0247-FEDER-039893.

This work was developed within the scope of the project CICECO-Aveiro Institute of Materials, UIDB/50011/2020, UIDP/50011/2020 & LA/P/0006/2020, financed by national funds through the FCT/MEC (PIDDAC). This work was also developed within the scope of the projects TEMA - Centre for Mechanical Technology and Automation, UID/EMS/00481/2019-FCT, CEECIND/01192/2017 and CENTRO-01-0145-FEDER-022083.

References

[1] Singh G, Verma A. A Brief Review on injection moulding manufacturing process. Mater Today Proc 2017;4:1423–33.

[2] Park C, Kim J, Sim A, Park I, Jang H, Chun E-J. Influence of high-power diode laser heat treatment on wear resistance of a mold steel. J Mech Sci Technol 2019;33:829–36.

[3] Lagarinhos JN, Afonso D, Torcato R, Santos C, Oliveira M. Effect of laser heat treatments on the hardness of tool steels. IOP Conf. Ser. Mater. Sci. Eng., vol. 1193, IOP Publishing; 2021, p. 12026.

[4] Syed B, Shariff SM, Padmanabham G, Lenka S, Bhattacharya B, Kundu S. Influence of laser surface hardened layer on mechanical properties of re-engineered low carbon steel sheet. Mater Sci Eng A 2017;685:168–77.

[5] Guarino S, Barletta M, Afilal A. High Power Diode Laser (HPDL) surface hardening of low carbon steel: Fatigue life improvement analysis. J Manuf Process 2017;28:266–71.

[6] Chun E-J, Sim A, Kim M-S, Kang N. Microstructural characterization of surface softening behavior for Cu-bearing martensitic steels after laser surface heat treatment. Metals (Basel) 2018;8:470.

[7] Shin W-S, Yoo HJ, Kim JH, Choi J, Chun E-J, Park C, et al. Effect of Laser Heat-Treatment and Laser Nitriding on the Microstructural Evolutions and Wear Behaviors of AISI P21 Mold Steel. Metals (Basel) 2020;10:1487.

[8] Li R, Jin Y, Li Z, Qi K. A comparative study of high-power diode laser and CO 2 laser surface hardening of AISI 1045 steel. J Mater Eng Perform 2014;23:3085–91.

[9] Soriano C, Leunda J, Lambarri J, Navas VG, Sanz C. Effect of laser surface hardening on the microstructure, hardness and residual stresses of austempered ductile iron grades. Appl Surf Sci 2011;257:7101–6.

[10] Choi S-D, Cheong S-H, Kim G-M, Yang S-C, Kim J-G. Characteristics of metal surface heat treatment by diode laser. J Korean Soc Manuf Process Eng 2007;6:16–23.

[11] Boztepe E, Alves AC, Ariza E, Rocha LA, Cansever N, Toptan F. A comparative investigation of the corrosion and tribocorrosion behaviour of nitrocarburized, gas nitrided, fluidized-bed nitrided, and plasma nitrided plastic mould steel. Surf Coatings Technol 2018;334:116–23.

[12] Wen DC. Microstructure and corrosion resistance of the layers formed on the surface of precipitation hardenable plastic mold steel by plasma-nitriding. Appl Surf Sci 2009;256:797–804.

[13] Sarkar S, Gopinath M, Chakraborty SS, Syed B, Nath AK. Analysis of temperature and surface hardening of low carbon thin steel sheets using Yb-fiber laser. Surf Coatings Technol 2016;302:344–58.

[14] Carpene E. Excimer laser treatments of iron, aluminum and silicon substrates in nitrogen and methane atmospheres. Univ Göttingen, Ger 2002.

[15] Maharjan N, Zhou W, Wu N. Direct laser hardening of AISI 1020 steel under controlled gas atmosphere. Surf Coatings Technol 2020;385:125399.

[16] Afir U. Steel 2311 - DIN 1.2311. 2021.

[17] Chen JY, Xue L. Microstructural characteristics of laser-clad AISI P20 tool steel. Proc. 1st Int. Surf. Eng. Congr. 13th IFHTSE Congr. Mater. Park ASM Int., 2002, p. 198.

[18] Kim JW, Choi JW, Lee DB. Characterization of oxide scales formed on low carbon steel between 1100 and 1250° C in air. Met Mater Int 2005;11:131–4.

[19] Maharjan N, Zhou W, Zhou Y, Wu N. Influence of operating parameters on morphology of laser hardened surfaces. High-Power Laser Mater. Process. Appl. Diagnostics, Syst. VII, vol. 10525, International Society for Optics and Photonics; 2018, p. 105250M.

[20] Rasband WS. ImageJ 1997.

[21] Santos LS dos. Influência da rugosidade na absorção de laser para tratamento de superficie metálica 2019.